Conference Paper, Published Version

Li, Jiaze; Claude, Nicolas; Tassi, Pablo; Cordier, Florian; Crosato, Alessandra; Rodrigues, Stéphane

Implementation of a novel approach accounting for the influence of vegetation on sediment transport in GAIA

Implementation of a novel approach accounting for the influence of vegetation on sediment transport in GAIA

Jiaze Li[1,2,5], Nicolas Claude[3], Pablo Tassi[1,2], Florian Cordier[1], Alessandra Crosato[4], Stéphane Rodrigues[5]
[1]National Hydraulics and Environment Laboratory (LNHE), EDF R&D, Chatou, France
2 Saint-Venant Hydraulics Laboratory (LHSV), ENPC, Cerema, EDF R&D, Chatou, France
3Centre d'Ingénierie Hydraulique, EDF, La Motte Servolex, France
4 Department of Water Resources and Ecosystems, IHE-Delft, Delft, Pays-Bas
5 UMR CNRS 7324 CITERES – Polytech Tours, Tours, France

***Abstract* — The influence of vegetation on flow and sediment transport is commonly accounted in 2D, horizontal, depth-averaged (2DH) models through the parameterization of a friction coefficient or by a drag force term in the momentum equations. In this study, we propose to implement a novel approach based on the work of Armanini and Cavedon (2019) and Bonilla Porras *et al.* (2020) to consider the effects of vegetation on flow and sediment transport. Combined with a drag force term implemented in the hydrodynamics equations, the initiation of motion parameter (Shields) was modified in the brand new sediment transport module GAIA to directly incorporate the effects of vegetation on sediment transport. A 2DH model is set-up and calibrated based on the flume experiments of Armanini & Cavedon (2019). Numerical results agree with the experimental data, but with less accuracy for high vegetation density. To validate the performance of this new approach, more numerical tests should be carried out on the basis of an independent set of physical experiments.**

I. INTRODUCTION

Anthropic activities such as channelization, sediment dredging, and dam building have affected many river systems worldwide. As a result of anthropogenic activities, channelized rivers generally show an increase of their base flow and a decrease of their flood frequency and magnitude. Consequently, reduced bar submersion and riverbed reworking have been observed in numerous regulated rivers worldwide, which might favor the expansion of vegetation over bars and inside channels (Figure 1). Vegetation increases the local hydraulic roughness as well as fine sediment deposition and reinforces the bed cohesion by the presence of roots systems [1]. Water levels increase due to the higher flow resistance and the smaller channel width, leading to an increased flood risk.

Numerous numerical models have been recently developed to consider the effects of vegetation on river morphodynamics. The commonly adopted approach to account for vegetation effects on flow resistance in two-dimensional, horizontal, depth-averaged models (2DH) is to define either a friction coefficient [2, 3, 4], or a drag force F_d added as a friction source term in the momentum equation [5, 6]. By doing so, the effect of vegetation on sediment transport is accounted indirectly by a reduced depth-averaged velocity. However, Yager & Schmeeckle [7] found that existing formulas commonly adopted to parameterize the bedload flux are inaccurate to reproduce observed solid discharge values in vegetated reaches.

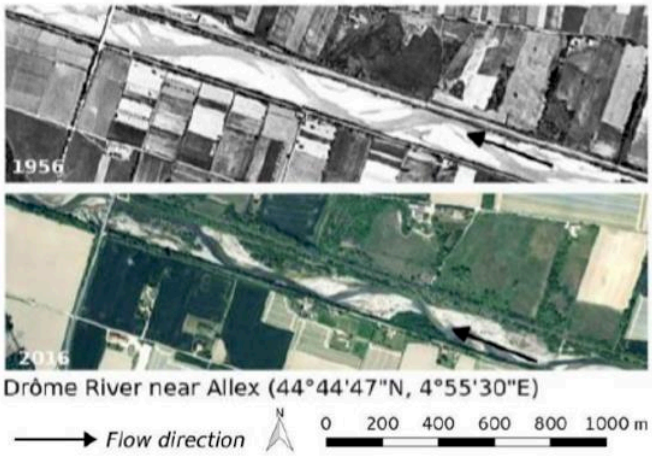

Figure 1: Examples of channelized gravel bed rivers located in the French Alpine region between 1956 and 2016, showing the development of vegetation on alternate bars (source: IGN) [5]

In their recent study, Armanini & Cavedon [8] proposed a novel approach that considers the effects of emergent vegetation on bedload transport by modifying Einstein's flow intensity parameter Ψ (Equation 5) with a correction factor that includes the plant characteristics. As a follow-up to the work of [8], Bonilla Porras *et al.,* [9] proposed an extension of this parameter to include submerged vegetation effects (Equation 6).

In this study, a modification of the dimensionless incipient grain mobility parameter is implemented in the sediment transport and bed evolution module GAIA. A 2DH model is set up using the open TELEMAC-MASCARET system. This consists of the hydrodynamic module TELEMAC-2D coupled with GAIA. The numerical results are compared with the experimental observations by Armanini & Cavedon [8] to test the implementation.

II. SEDIMENT TRANSPORT THROUGH VEGETATION

Two dimensionless parameters are usually proposed to describe the fundamental principles of most commonly bed-load

transport equations [10], namely the dimensionless sediment transport rate, Φ,

$$\Phi = \frac{q_s}{d\sqrt{g\Delta d}} \quad (1)$$

and the flow intensity parameter, Ψ,

$$\Psi = \frac{g\Delta d}{u_*^2} \quad (2)$$

where q_s is the sediment transport rate per unit width (m^2/s); d is the representative sediment particle size (m); $\Delta = (\rho_s - \rho_w)/\rho_w$ is the submerged relative density of sediment (-), with ρ_s and ρ_w respectively the sediment and fluid density; g is the gravitational acceleration (m/s^2); and u_* is the shear velocity (m/s).

The dimensionless sediment transport rate Φ can be expressed as a function of the flow intensity parameter:

$$\Phi = f(\Psi) = f(\theta^{-1}) \quad (3)$$

where θ is the Shields parameter and $\theta = \frac{1}{\Psi}$.

A. Bedload through emergent vegetation

Derived from momentum balance analysis, a modification of Equations (1) and (2) is proposed by Armanini & Cavedon [8] to include the effects of emergent vegetation.

The dimensionless sediment transport rate in vegetated beds is defined as follows:

$$\Phi_v = \frac{q_s}{d\sqrt{g\Delta d}}(1 - \alpha_\Omega \Omega_v) \quad (4)$$

where Ω_v is the areal density of plant (-) and α_Ω is a calibration factor (-). This modification takes account of the reduction of the active exchange surface between the bed and the flow [8].

The flow intensity parameter in vegetated beds is computed as follows:

$$\Psi_v = \Psi\left(1 + \beta_v \Omega_v \frac{h}{D_v}\left(\frac{h}{d}\right)^{b_v}\right) \quad (5)$$

where h is the water depth (m), D_v is the plant stem diameter (m), and β_v and b_v are calibration parameters (-).

B. Bedload through submerged vegetation

Bonilla Porras *et al.*, [9] reworked the momentum balance analysis with submerged vegetation and proposed an updated version of the flow intensity parameter that adapts both to emergent and submerged vegetation, as follows:

$$\Psi_v = \Psi\left(1 + \beta_v \Omega_v \frac{h_v}{D_v}\left(\frac{h}{d}\right)^{b_v}\left(\frac{h_v}{h}\right)^{\gamma_v}\right) \quad (6)$$

where h_v (m) is the effective plant height (equals to water depth for emergent vegetation), γ_v is calibration factor (-).

The calibration of parameters β_v, b_v and γ_v is based on a series of flume tests carried out at the Hydraulics Laboratory at the University of Trento (Italy). The line of best fit equation is:

$$\Psi_v = \Psi(1 + K_v \Omega_v \frac{h_v}{D_v}) \quad (7)$$

in which $K_v = 49.38\left(\frac{h_v}{h}\right)^{-0.92} - 10.97\left(\frac{h_v}{h}\right)^{-1.92}$.

III. Numerical Implementation

In this study, we implemented the approach of Armanini & Cavedon's [8] and Bonilla Porras *et al.* [9] into GAIA to consider the direct effect of vegetation on sediment transport. As shown in Figure 2, the implementation can be achieved by adding a drag force in shallow water equations to account for the effect of vegetation on hydrodynamics and by modifying the Shields parameter θ to incorporate the effect of vegetation on morphodynamics.

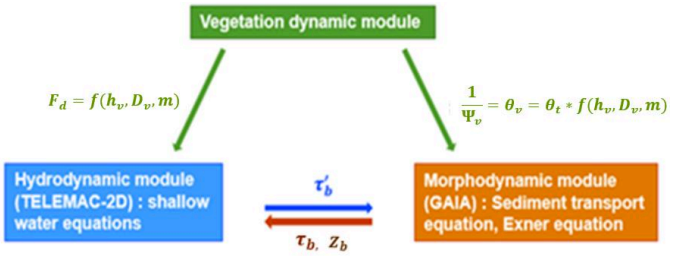

Figure 2: Schematization of the way we account for the interactions between vegetation, water flow and sediment transport for the morphodynamic modeling, τ_b is the bed shear stress, τ_b' is the shear stress due to skin friction, Z_b is the bed elevation.

Both the drag force and the modified Shields parameter are functions of the flow parameters and the vegetation parameters (i.e., plant diameter, height, and density).

A. Drag force in TELEMAC-2D

The effects of vegetation on hydrodynamics can be represented by a friction coefficient. However, Hervouet [11] indicated that by simply giving a specific friction coefficient to simulate the effect of vertical structures like vegetation, the last is not applied correctly. Hence, to represent the effect of vegetation, a drag force is added to the momentum equations according to [5], as follows:

$$F_d = -\frac{1}{2} C_d \rho_w \alpha_v m D_v \min(h_v, h)|U_v|U_v \quad (8)$$

where F_d is the drag force (N), C_d is the drag coefficient (-), ρ_w is the water density (kg/m^3), α_v is a shape factor equal to 1 for rigid cylinders (-), U_v is the flow velocity acting on vegetation (m/s), m is the number of stems per unit area (-), D_v is the stem diameter (m), and h_v is the plant height (m).

For emergent vegetation, U_v is equal to the depth-averaged velocity. For submerged vegetation, U_v is determined by the formula of Stone and Shen [12] as follows:

$$U_v = \eta_v U\left(\frac{h_v}{h}\right)^{\frac{1}{2}} \quad (9)$$

where η_v is a coefficient and $\eta_v = \frac{(1 - Dm^{0.5})}{(1 - \frac{h_v}{h} Dm^{0.5})}$

A sketch of the Fortran code implemented to compute the drag force is presented in Figure 3.

```
!*********************************************************************
! NPOIN:   Number of computational nodes
! INPOLY:  Function to determine whether a given point is inside the polygon
! HN:      Water depth
! UN:      Velocity along X
! VN:      Velocity along Y
! H_VEG:   Vegetation height
! D_VEG:   Stem diameter
! M_VEG:   Number of stems per unit area
! FUDRAG:  Drag force along X
! FVDRAG:  Drag force along Y
! CD:      Drag coefficient
!*********************************************************************
!---------------------------------------------------------------------
DO I=1,NPOIN
   IF (HN%R(I).GT.0D0) THEN
      RATIO_VEG   = MIN(HN%R(I),H_VEG)/HN%R(I)
      ETA_VEG     = (1.0-D_VEG*SQRT(M_VEG))/(1.0-D_VEG*SQRT(M_VEG)*RATIO_VEG)
      UNORM       = SQRT(UN%R(I)**2+VN%R(I)**2)*ETA_VEG*SQRT(RATIO_VEG)
      FUDRAG%R(I) = -0.5D0*D_VEG*M_VEG*CD*UNORM*RATIO_VEG
      FVDRAG%R(I) = -0.5D0*D_VEG*M_VEG*CD*UNORM*RATIO_VEG
   ENDIF
ENDDO
!---------------------------------------------------------------------
```

Figure 3: Sketch of Fortran code used to calculate the drag force (dragfo.f)

B. *Modification of the Shields parameter θ in GAIA*

The implementation of equation (7) is accomplished through the modification of the Shields parameter θ. Figure 4 presents a conceptual diagram with the procedure followed to compute the modified Shields parameter θ_v.

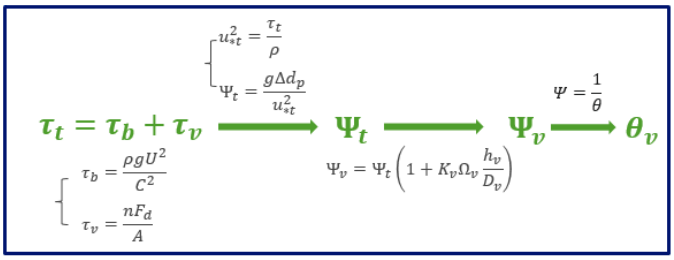

Figure 4: Chronological steps for the calculation of θ_v

For each symbol, the subscripts b, v, t stand for "bed", "vegetation" and "total", respectively. From the momentum balance analysis, the total shear stress τ_t is equal to the sum of the bed shear stress τ_b and the drag stress of vegetation exerted on the fluid τ_v, which is calculated from the drag force (Equation 8). The total flow intensity parameter Ψ_t is then computed from the total shear velocity u_{*t}, which is in turn a function of τ_t. By using equation (7), the modified flow intensity parameter for vegetated beds Ψ_v is obtained.

A sketch of the Fortran code implemented to compute the modified Shields parameter is presented in Figure 5.

```
!*********************************************************************
! NPOIN:   Number of computational nodes
! INPOLY:  Function to determine whether a given point is inside the polygon
! HN:      Water depth
! UN:      Velocity along X
! VN:      Velocity along Y
! H_VEG:   Vegetation height
! D_VEG:   Stem diameter
! M_VEG:   Number of stems per unit area
! DEN_VEG: Areal density of vegetation
! FUDRAG:  Drag force along X
! FVDRAG:  Drag force along Y
! CD:      Drag coefficient
! MU:      Skin friction coefficient
! TOB:     Total bed shear stress
! XMVE:    Fluid density
!*********************************************************************
!---------------------------------------------------------------------
DO I=1,NPOIN
   IF (HN%R(I).GT.0D0.AND.AND.UNORM%R(I).GT.0D0) THEN
!-----------Calculation of Tau_v/water density-----------------------
      RATIO_VEG = MIN(HN%R(I),H_VEG)/HN%R(I)
      ETA_VEG = (1.0-D_VEG*SQRT(M_VEG))/(1.0-D_VEG*SQRT(M_VEG)*RATIO_VEG)
      PART_V = 0.5D0*CD*D_VEG*M_VEG*MIN(HN%R(I),H_VEG
      &        *(UNORM%R(I)**2)*(ETA_VEG**2)*RATIO_VEG
!-----------Calculation of Tau_b/water density-----------------------
      PART_S = MU%R(I)*TOB%R(I)/XMVE
!-----------Calculation of total shear velocity----------------------
      USTAR_T2 = (PART_V+PART_S)
!-----------Calculation of total flow intensity parameter Psi_t------
      PSI_T = CONS2/USTAR_T2
!-----------Calculation of modified flow intensity parameter Psi_v-----
      KV = 49.38*(RATIO_VEG**(-0.92))-10.97*(RATIO_VEG**(-1.92))
      FACTOR = 1.0+KV*DEN_VEG*MIN(HN%R(I),H_VEG)/D_VEG
      PSI_V = PSI_T*FACTOR
!-----------Calculation of modified Shields--------------------------
      TETAP%R(I) = 1.0/PSI_V
   ENDIF
ENDDO
!---------------------------------------------------------------------
```

Figure 5: Sketch of Fortran code used to compute the modified Shields parameter

IV. NUMERICAL MODEL TESTING

To verify the numerical implementations in GAIA, a 2D morphodynamic model is set-up and run to reproduce the flume experiments by Armanini & Cavedon [8].

A. *Flume experiment of Armanini & Cavedon [8]*

Physical experiments were carried out in a 15 m long and 0.50 m wide rectangular flume. Two types of cylindrical elements were used to represent vegetation: aluminium cylinders with an average diameter of 1 cm; and rigid plastic cylinders with an average diameter of 3 cm, set in staggered configurations. Four distinct zones divide the channel longitudinally, as shown in Figure 6. The first three zones A, B and C are associated with three different vegetation densities of 200, 100 and 50 plants/m^2 respectively, and the downstream zone D corresponds to a plant-free area. Complementary scenarios with a single vegetation partition (200 plants/m^2) and totally plant-free area were also carried out.

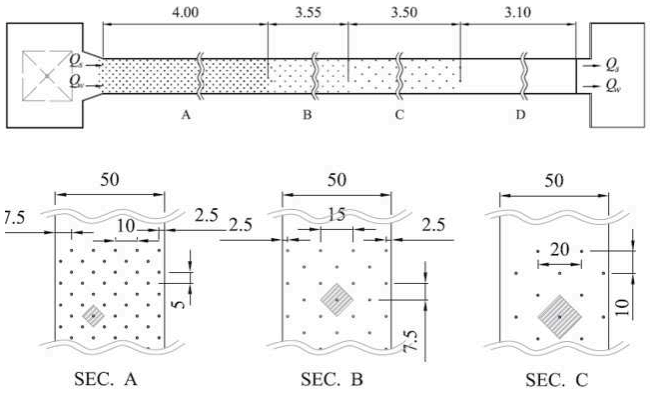

Figure 6: Flume vegetation areas: (A) reach with dense configuration (200 plants/m^2), (B) reach with intermediate density (100 plants/m^2), (C) reach with sparse configuration (50 plants/m^2), D) vegetation-free reach. (reproduced from Armanini & Cavedon (2019) [8])

The experiments were run under stationary conditions (constant water discharge and constant sediment discharge). Two types of sediments were used: fine uniform sand ($\rho_s = 2591\ kg/m^3$ and $d_{50} = 0.5\,mm$) and artificial spherical plastic particles ($\rho_s = 1050\ kg/m^3$ and $d_{50} = 0.55\,mm$). The water discharge Q, the sediment transport rate Q_s, the water surface and the bed level were measured during the experiment. All the experiments were carried out under steady and uniform flow conditions, in which the morphodynamic equilibrium was guaranteed at the end of the experimental runs.

In this work, only experimental runs with subcritical flows regime (Fr < 1) and uniform sediment (sand) were selected, as shown in Tables 1 and 2.

Name	Number of stem per m^2	Vegetation density (-)	Water discharge Q (m^3/s)	Sediment discharge Q_s (m^3/s)	Plant diameter $D_v(m)$	Water depth h (m)	Free surface slope i $(-)$
1.R20	200	0.0157	0.020	1.45E-06	0.01	0.155	0.0080
	100	0.0073			0.01	0.136	0.0044
	50	0.0039			0.01	0.127	0.0037
	0	0			0	0.102	0.0014
2.R9	200	0.0157	0.009	4.68E-08	0.01	0.115	0.0049
	100	0.0073			0.01	0.097	0.0026
	50	0.0039			0.01	0.093	0.0018
	0	0			0	0.080	0.0008
3.R10	200	0.0157	0.010	1.96E-07	0.01	0.111	0.0056
	100	0.0073			0.01	0.099	0.0028
	50	0.0039			0.01	0.098	0.0023
	0	0			0	0.076	0.0010
NP1-NV	200	0.0157	0.010	3.65E-08	0.01	0.112	0.0050
	100	0.0073			0.01	0.096	0.0026
	50	0.0039			0.01	0.088	0.0020
	0	0			0	0.078	0.0011
NP2-NV	200	0.0157	0.020	1.30E-06	0.01	0.132	0.0101
	100	0.0073			0.01	0.110	0.0056
	50	0.0039			0.01	0.100	0.0037
	0	0			0	0.092	0.0019

TABLE 1: EXPERIMENTAL CONDITIONS OF THE SCENARIOS WITH 4 DISTINCT VEGETATION AREAS RETAINED FOR THE NUMERICAL SIMULATIONS (ADAPTED FROM ARMANINI & CAVEDON [8])

Name	Number of stem per m^2	Vegetation density (-)	Water discharge Q (m^3/s)	Sediment discharge Q_s (m^3/s)	Plant diameter $D_v(m)$	Water depth h (m)	Free surface slope i $(-)$
1.F20.8	200	0.0157	0.021	1.91E-06	0.01	0.157	0.0092
1.M20-FITTA	200	0.0157	0.020	2.33E-05	0.01	0.091	0.02668
2.M25-FITTA	200	0.0157	0.025	5.20E-05	0.01	0.099	0.03452
3.M23-FITTA	200	0.0157	0.023	8.68E-05	0.01	0.081	0.04275
4.F25	200	0.0157	0.025	6.35E-05	0.01	0.092	0.03823
4.M20-2-Fitta	200	0.0157	0.020	3.28E-06	0.01	0.138	0.0112
4.R25	200	0.0157	0.025	9.84E-05	0.01	0.090	0.0454
5.F20	200	0.0157	0.020	8.32E-05	0.01	0.070	0.04223
6.F20-2	200	0.0157	0.020	1.60E-05	0.01	0.105	0.02071

TABLE 2: EXPERIMENTAL CONDITIONS OF THE SCENARIOS WITH A SINGLE VEGETATION AREA RETAINED FOR THE NUMERICAL SIMULATIONS (ADAPTED FROM ARMANINI & CAVEDON [8])

B. *Model set-up and testing*

The numerical model scales 1:1 the prototype. An unstructured triangular numerical mesh of 0.05 m is used, consisting of 3360 nodes and 6072 elements. A vegetation-free zone was assigned from 0 to 0.825 m along the x-axis. The upstream boundary conditions correspond to the experimental constant flow and solid discharges, and the imposed downstream water level is estimated from the measured water surface slope. The drag coefficient is set equal to 1 according the shape and rigidity of the cylinders. Only the bedload sediment transport mechanism is considered in this study. The van Rijn [13] sediment transport formula is adopted here as it is valid for finer material in the range $d = (0.2 - 2)\,mm$. The critical Shields parameter is calculated according to Brownlie [14], as:

$$\theta_{cr} = 0.22 * D_*^{-0.9} + 0.06e^{-7.73D_*^{-0.9}} \quad (9)$$

where $D_* = d(g\Delta/\nu^2)^{1/3}$ is dimensionless particle diameter (-), with ν the kinematic viscosity (m^2/s).

The Strickler coefficient is used as friction coefficient to account for the bottom roughness. The adopted value is based on three no-vegetated scenarios shown in Table 3, where the average value of 61 $m^{1/3}/s$ is retained from the calibration procedure.

Name	Water discharge Q (m^3/s)	Sediment discharge Q_s (m^3/s)	Sediment density (kg/m^3)	Particle size $d_p(m)$	Water depth h (m)	Free surface slope i $(-)$	**Calibrated Strickler K $(m^{1/3}/s)$**
6.F20-2	0.020	1.60E-05	2591	0.0005	0.060	0.00525	**69**
2.M25	0.020	5.20E-05	2591	0.0005	0.056	0.00897	**59**
4.M20-2	0.020	3.28E-06	2591	0.0005	0.091	0.00144	**57**

TABLE 3: STRICKLER COEFFICIENT CALIBRATION BASED ON THREE NO-VEGETATION SCENARIOS

C. *Numerical results*

Figure 7 shows an example of bed elevation obtained at the end of the numerical simulation of scenario 1.R20 without and with the implementation of the modified Shields parameter θ_v.

The abrupt changes of bed elevation observed in the Armanini & Cavedon's experiences are well reproduced by the newly implemented model (Figure 8). This behaviour observed in the transition zones between three vegetated areas and one vegetation-free area were unable to be captured by the original model.

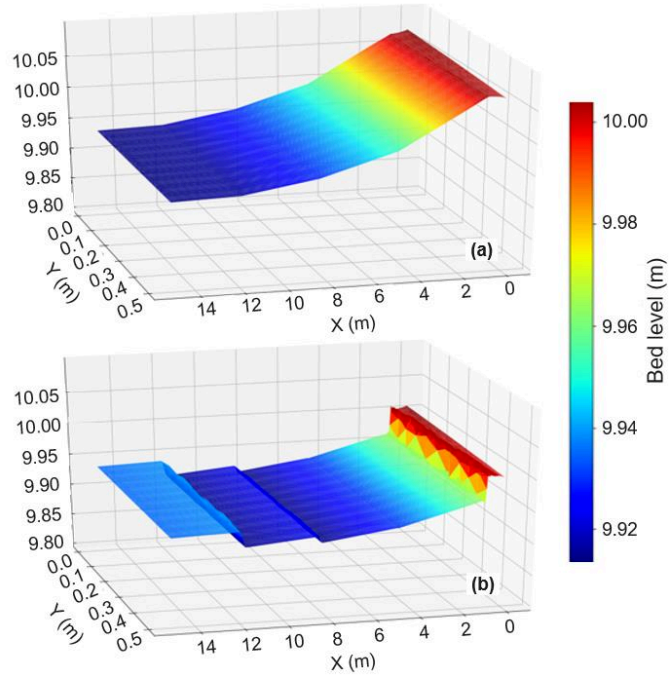

Figure 7: Bed elevation obtained at the end of simulation 1.R20: (a) original model without implementation of θ_v, (b) modified model with implementation of θ_v (arrow indicates flow direction).

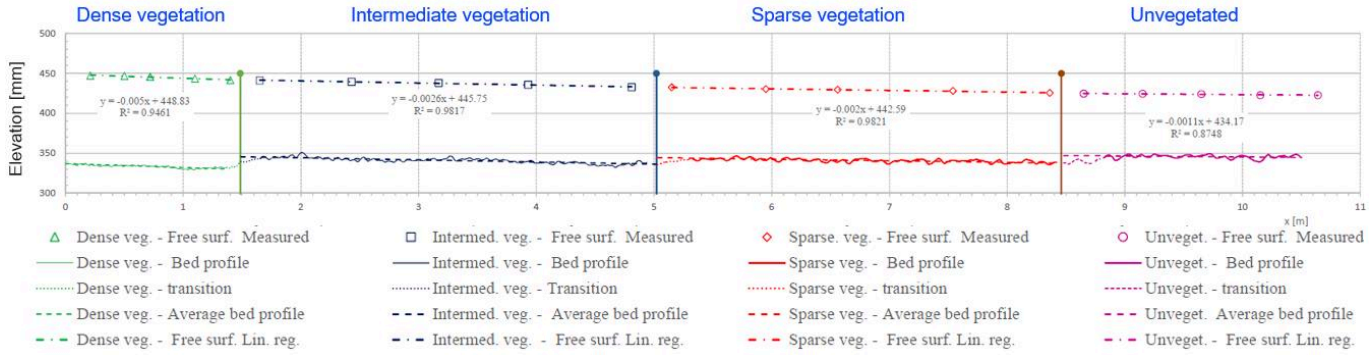

Figure 8: Measured longitudinal profiles of bed elevation and free surface of scenario NP1 (source: Armanini & Cavedon [8])

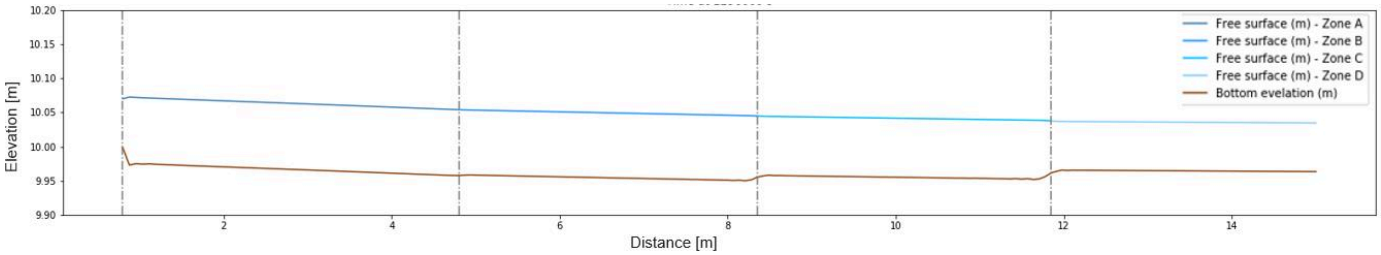

Figure 9: Numerical longitudinal profiles of bed elevation and free surface of scenario NP1 (extracted along y=0.25 m)

Figures 8 and 9 present the measurements and numerical results of the longitudinal profile of free surface and bed elevation at steady-state conditions, respectively. The free surface profile and bed level slope being parallel in each vegetated area indicates that the numerical model is under steady and uniform conditions, same than the experiment [15]. For high vegetation density, Ω_v, the numerical results show an increase in water depth, h, and an increase in the free surface and bed slopes, i, which is consistent with observations.

Scenario	Number of stem per m^2	Measured water depth (m)	Simulated water depth (m)
1R20	200	0.155	0.137
	100	0.136	0.137
	50	0.127	0.125
	0	0.102	0.096
2R9	200	0.115	0.085
	100	0.097	0.084
	50	0.093	0.076
	0	0.080	0.065
3R10	200	0.111	0.086
	100	0.099	0.084
	50	0.098	0.076
	0	0.076	0.065
NP1	200	0.112	0.097
	100	0.096	0.095
	50	0.088	0.086
	0	0.078	0.071
NP2	200	0.132	0.140
	100	0.110	0.139
	50	0.100	0.127
	0	0.092	0.097

TABLE 4: COMPARISON OF MEASURED AND SIMULATED WATER DEPTH OF THE SCENARIOS WITH 4 DISTINCT VEGETATION AREAS

However, the distinction between dense (200 plant/m^2) and intermediate vegetation (100 plant/m^2) are not as evident as observed in experiments. Table 4 shows the experimental data and the numerical results of water depth for all the scenarios with 4 distinct vegetation areas. The average difference in water depth between dense and intermediate vegetation areas is 0.017 m in the experiments, but only 0.001 m in the model, which barely show distinction.

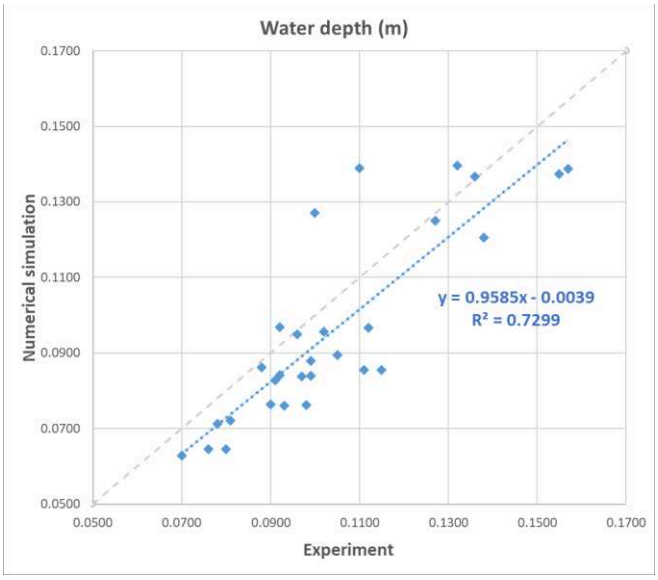

Figure 10: Comparison of the water depths obtained in the numerical model vs. in the experiment at morphodynamical equilibrium

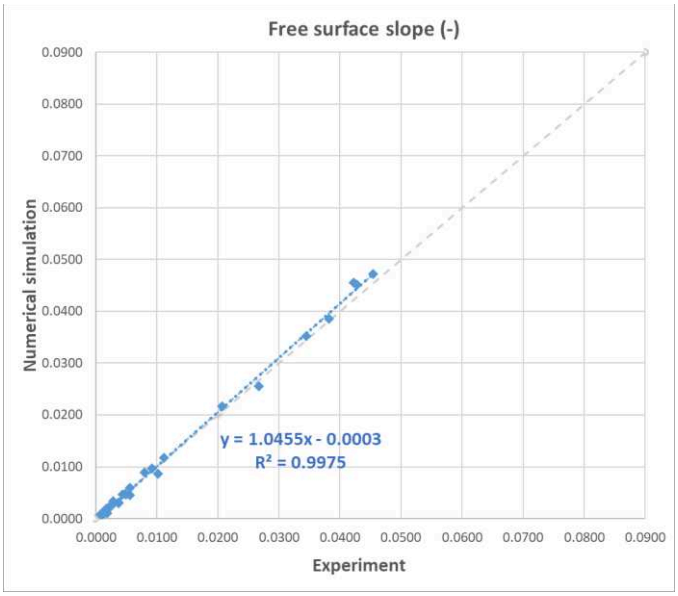

Figure 11: Comparison of the free surface slope (same as bed slope) obtained in the numerical model vs. in the experiment at morphodynamics equilibrium

Figures 10 and 11 show the comparison of numerical results and experimental observations in terms of water depth and free surface (bed) slope, for all scenarios (Tables 1 and 2). The model is able to reproduce correctly the experimental observations, which is represented by a high correlation coefficient R^2 of 0.73 and 0.99, a linear function slope of 0.958 and 1.0455, respectively.

V. CONCLUSIONS AND PERSPECTIVES

Derived from the momentum balance analysis, Armanini & Cavedon [8] proposed a novel approach to include the effects of emerging vegetation on bed load rates by adapting the dimensionless sediment transport rate Φ_v and the flow intensity parameter Ψ_v. Subsequently, Bonilla Porras *et al.* [9] extended this modification to include also submerged vegetation.

The present study implemented this latter approach in GAIA by modifying the Shields parameter θ. The numerical model was tested on the basis of the flume experiment of Armanini & Cavedon [8], with the aim of verifying its implementation in the TELEMAC-MASCARET modelling system. Each simulation reached morphodynamic equilibrium, well reproducing the experiments. By comparing water depth and free surface slopes, numerical results agree with the experimental observations. However, the numerical model seems to have limitations for dense vegetation (200 plants/m^2). More numerical tests should be carried out on independent data sets to validate the performance of this approach for high-density and emergent/submerged vegetation conditions.

ACKNOWLEDGEMENT

The present work is based on previous research of Armanini & Cavedon (2019) and Bonilla Porras *et al.,* (2020). The authors kindly acknowledge Prof. Aronne Armanini, Valentina Cavedon and José Antonio Bonilla Porras for the rich discussions and for providing the experimental data used in this work.

REFERENCES

[1] Gurnell, A. M., Bertoldi, W., & Corenblit, D. (2012). Changing river channels: The roles of hydrological processes, plants and pioneer fluvial landforms in humid temperate, mixed load, gravel bed rivers. *Earth-Science Reviews*, *111*(1-2), 129-141.

[2] Baptist M.J. 2005. Modelling floodplain biogeomorphology. PhD Thesis, Delft University of Technology, ISBN 90-407-2582-9.

[3] Crosato, A., & Saleh, M. S. (2011). Numerical study on the effects of floodplain vegetation on river planform style. *Earth Surface Processes and Landforms*, *36*(6), 711-720.

[4] Vargas-Luna, A., Crosato, A., & Uijttewaal, W. S. (2015). Effects of vegetation on flow and sediment transport: comparative analyses and validation of predicting models. *Earth Surface Processes and Landforms*, *40*(2), 157-176.

[5] Jourdain, C., Claude, N., Tassi, P., Cordier, F., & Antoine, G. (2020). Morphodynamics of alternate bars in the presence of riparian vegetation. *Earth Surface Processes and Landforms*, *45*(5), 1100-1122.

[6] C.A.M.E. Wilson, O. Yagci, H. ‐ P. Rauch & T. Stoesser (2006) Application of the drag force approach to model the flow ‐ interaction of natural vegetation, International Journal of River Basin Management, 4:2, 137-146, DOI: 10.1080/15715124.2006.9635283

[7] Yager, E. M., & Schmeeckle, M. W. (2013). The influence of vegetation turbulence and bed load transport. *Journal of Geophysical Research: earth Surface*, *118*(3), 1585-1601.

[8] Armanini, A., & Cavedon, V. (2019). Bed-load through emergent vegetation. *Advances in Water Resources*, *129*, 250-259.

[9] Bonilla Porras, J.A., Armanini, A., & Crosato, A., (2020) Sediment transport through submerged vegetation. River Flow 2020 (Delft, Netherlands) In: Uijttewaal et a. (Eds), River Flow 2020, Taylor & Francis Group: London2020, p. 1-8

[10] Einstein, H. A. (1950). *The bed-load function for sediment transportation in open channel flows* (No. 1026). US Government Printing Office.

[11] Hervouet, J. M. (2007). *Hydrodynamics of free surface flows: modelling with the finite element method* (Vol. 360). Chichester, UK: Wiley.

[12] Stone, B. M., and H. T. Shen (2002), Hydraulic resistance of flow in channels with cylindrical roughness, Journal of Hydraulic Engineering, 128(5), 500-506.

[13] Van Rijn, L. C. (1984). Sediment transport, part I: bed load transport. *Journal of hydraulic engineering*, *110*(10), 1431-1456.

[14] Brownlie, W. R. (1981). Prediction of flow depth and sediment discharge in open channels.

[15] Bolla Pittaluga, M., Luchi, R., and Seminara, G. (2014), On the equilibrium profile of river beds, J. Geophys. Res. Earth Surf., 119, 317–332, doi:10.1002/2013JF002806.